Aligning Families of Two-Dimensional Gels by a Combined Multiresolution Forward-Inverse Transformation Approach

FLORIAN A. POTRA[1] and XING LIU[2]

ABSTRACT

A new method for aligning families of two-dimensional polyacrylamide gel electrophoresis (2D-PAGE) images arising in proteomics studies is presented. Forward piecewise bilinear transformations are used to determine an ideal gel and to obtain an initial alignment of the family of gels to this ideal gel. Both the ideal landmarks and the coefficients defining the transformations are obtained by solving a quadratic programming problem. The alignment is then improved by using inverse transformations on finer grids. Numerical results for a family of 123 gels are reported.

Key words: proteomics 2D-PAGE, image alignment, image registration multi-resolution, interior-point method.

1. INTRODUCTION

PROTEOMICS, the study of proteomes, is the large-scale analysis of complex protein mixtures focusing on the qualitative and quantitative variations of protein expression levels.

A typical proteomics study involves separation, visualization, and analysis of complex mixtures containing as many as several thousand proteins obtained from whole cells, tissues, or organisms. Two-dimensional polyacrylamide gel electrophoresis (2D-PAGE), first introduced by O'Farrell (1975) and Klose (1975), remains one of the core methods to simultaneously separate and quantitate up to 10,000 proteins (Dowsey et al., 2003). With this technique, proteins can be separated according to their isoelectric point and relative mass. The separated proteins are then stained (e.g., with fluorescent dyes) so that they are readily detectable, and the gels are digitally scanned into a database for storage.

One of the most important objectives of proteomics is to compare the differential expression between a family of gel images obtained from different groups (e.g., experimental and control groups, or health and disease-associated groups). Comparison of raw images is very difficult, since gels undergo substantial deformation during the preparation process. Even under strictly controlled laboratory conditions, repeated analysis of the same sample may produce non-identical gels (Salmi et al., 2002; Voss and Haberl, 2000). The distortions are due to the structure of the polyacrylamide net, the characteristics of the transporting solution, the solvent conditions, the nature of the electric field, and other factors.

---

[1]Department of Mathematics and Statistics, UMBC, 1000 Hilltop Circle, Baltimore, Maryland.
[2]NewDay Financial LLC, Eight Tower Bridge, 161 Washington Street, Conshohocken, Pennsylvania.

Figure 1 is a direct superimposition of two gel images. Overall location shifts and possible distortions (e.g., rotation, dilation) are obvious in the figure. To account for experimental variation, gels have to be aligned before doing any analysis for detecting the biological variation and the variation attributable to a treatment effect or exogenous stimulus like environmental changes.

Alignment of a family of gel images can be done by means of geometrical transformations (image warping methods) applied to the coordinate domain of the images (Dowsey et al., 2003; Glasbey and Mardia, 1998; Gustafsson et al., 2002). The transformed images should have no (or very little) geometrical variations, so that only statistical and biological variation are observed. Most image warping methods rely on some preassigned control points or landmarks, which are a relatively small group of spots present in all the gels being compared. They should be selected so that they are evenly distributed over the gel image. The number of the landmarks should be large enough, so that they can carry enough information, but not very large because this would increase computational complexity and may result in over-fitting. The shape and size of the protein spots chosen as landmarks can very significantly, but for the purpose of image warping only the x-y coordinates of their centers are important. Therefore, for the remainder of this paper we will consider that the landmarks are given by those coordinates.

Until recently, alignment of families of 2D gels was done by choosing one gel of the family as "target," and by constructing appropriate geometric transformations to map the other gels ("source" gels) into the target gel. Since for each source gel the corresponding transformation is determined by using only the information contained in the landmarks present in the source gel and the target gel, this (pair-wise) alignment approach can be implemented at a relatively low computational cost. However, the choice of a target gel, which is done by a human operator, may introduce a bias in the alignment process.
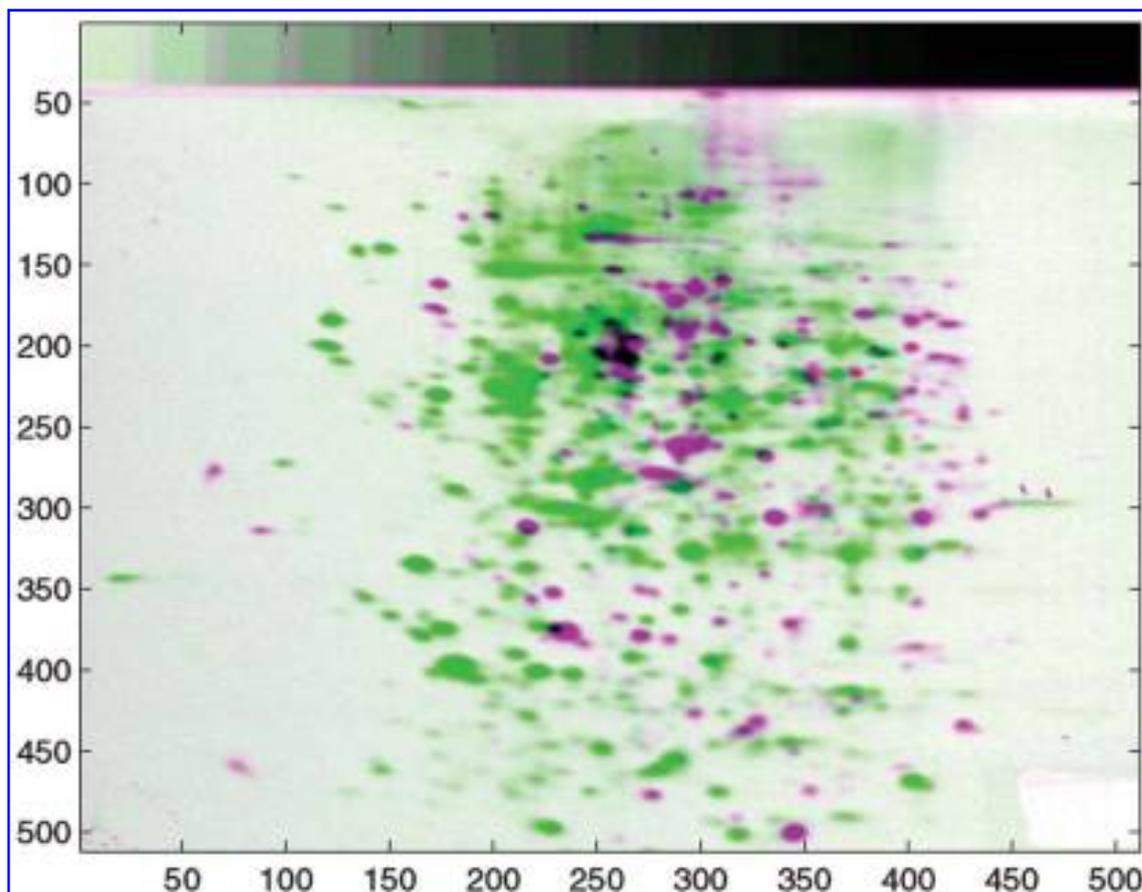
FIG. 1. Two gels from different treatment groups are superimposed. Overall location shift and local distortions can be clearly seen here.

Moreover the pair-wise alignment does not use any global information about the whole family of gels. In case the chosen target is an outlier or contains severe local distortions, the resulting alignment is very poor, or the algorithm may fail altogether.

In a recent paper (Potra et al., 2004), we have proposed a new approach for aligning families of 2D gels where the information contained in the landmarks of the whole family is used to create an ideal gel, and to determine transformations that optimally align all the gels of the family to this ideal gel. The ideal landmarks, along with the coefficients defining the transformations, are obtained as the solution of a large-scale quadratic programming problem, which can be efficiently solved with modern interior-point algorithms (Potra and Wright, 2000). Since both the coefficients defining the transformations and the ideal landmarks are unknowns, our approach can be efficiently implemented only with forward transformations which lead to optimization problems with linear constraints. However, as shown in Kaczmarek et al. (2003), the use of inverse transformations has certain advantages in assigning the intensity values of the pixels in the transformed image. Unfortunately, the use of inverse transformations in the framework of Potra et al. (2004) leads to nonlinear constraints, and this precludes the use of existing interior-point methods for quadratic programming.

In order to overcome the shortcomings of both forward and inverse transformations, in this paper we propose a new approach for aligning families of 2D gels. First, the locations of the ideal landmarks on the ideal gel, along with the approximate size of the ideal gel, are obtained as the solution of a large scale quadratic optimization problem. The quadratic programming problem can be efficiently solved by interior-point methods even for large families of gels. In the forward phase of our method, we use a relatively coarse grid. Inverse transformations are then constructed for each source gel by using a sequence of finer grids, which results in an improved alignment of the family. Both the forward and the inverse transformations are constructed in such a way that they are very likely to be one-to-one mappings. Moreover, because the domain considered in the inverse transformations is in the range of the forward transformations, there will be no pixels beyond the range of the inverse transformation. After obtaining the inverse transformation, we can assign intensities for all the pixels of the transformed source images, and the transformed images are well aligned. We describe the method in detail later in the paper.

We note that piecewise bilinear transformations on a hierarchical grid have been used before for pair-wise alignment of 2D gel images (Salmi et al., 2002; Veeser et al., 2001). Our approach differs in that we aim at aligning whole families of gels (as opposed to a pair), which leads to solving a constrained optimization problem rather than an unconstrained optimization problem. This large scale optimization problem is solved by state-of-the-art interior-point methods. We mention that in the present paper we use a different representation of the piecewise bilinear transformation than in Potra et al. (2004). More precisely, in the present paper the bilinear transformation on a subrectangle of the grid is represented by the values at the four vertices of the subrectangle, while in Potra et al. (2004) it is given by its coefficients. This way of representing the piecewise bilinear transformation, which is also used in Veeser et al. (2001) and Salmi et al. (2002), has the advantage that no equality constraints are needed to enforce continuity of the global warping functions. The only constraints that are imposed are the inequality constraints ensuring that the quadrilaterals after transformation do not overlap and that the resulting warping functions map the landmarks of the gel family into an arbitrarily small neighborhood of the ideal landmarks. The quadratic objective function is chosen in such a way that the resulting warping functions have minimum curvature and are as close as possible to the identity transformations. This produces an optimal alignment of the landmarks without introducing unnecessary deformations.

The precise description of our approach is given in Section 2. In Section 3, we evaluate the performance of the method on a small gel family, composed of 4 gels, and on a large family, composed of 123 gels. Some final conclusions are presented in Section 4.

2. PIECEWISE BILINEAR TRANSFORMATIONS USING HIERARCHICAL GRIDS

2.1. Forward transformations

Given M source gel images $\mathcal{I}^{(1)}, \mathcal{I}^{(2)}, \ldots, \mathcal{I}^{(M)}$, with N preassigned landmarks on each image, we denote by $L_{il} = (x_{il}, y_{il})^T$ the lth landmark on $\mathcal{I}^{(i)}$, $l = 1, \ldots, N$. We assume that $\mathcal{I}^{(i)}$ is included in the

rectangle $\Omega^{(i)} = [\check{\tau}_i^x, \hat{\tau}_i^x] \times [\check{\tau}_i^y, \hat{\tau}_i^y]$. This rectangle is divided into $p_i \times q_i$ equal sub-rectangles

$$\Omega_{jk}^{(i)} = \left\{ v = \begin{pmatrix} x \\ y \end{pmatrix} \in R^2, \, s_j^{(i)} \le x \le s_{j+1}^{(i)}, \, t_k^{(i)} \le y \le t_{k+1}^{(i)} \right\}, \, j = 1, \ldots, p_i, \, k = 1, \ldots, q_i, \quad (2.1)$$

with vertices $v_{jk}^{(i)} = (s_j^{(i)}, t_k^{(i)})^T$, where

$$s_j^{(i)} = \check{\tau}_i^x + (j-1)\Delta x^{(i)}, \, j = 1, \ldots, p_i + 1, \quad (2.2)$$

$$t_k^{(i)} = \check{\tau}_i^y + (k-1)\Delta y^{(i)}, \, k = 1, \ldots, q_i + 1, \quad (2.3)$$

and

$$\Delta x^{(i)} = \frac{\hat{\tau}_i^x - \check{\tau}_i^x}{p_i}, \quad \Delta y^{(i)} = \frac{\hat{\tau}_i^y - \check{\tau}_i^y}{q_i}. \quad (2.4)$$

On each sub-rectangle, we define a bilinear transformation $T_{jk}^{(i)} \colon \Omega_{jk}^{(i)} \to R^2$ as

$$T_{jk}^{(i)} \begin{pmatrix} x \\ y \end{pmatrix} = \begin{pmatrix} \alpha_{jk}^{(i)} x + \beta_{jk}^{(i)} y + \gamma_{jk}^{(i)} + \theta_{jk}^{(i)} xy \\ \delta_{jk}^{(i)} x + \varphi_{jk}^{(i)} y + \psi_{jk}^{(i)} + \zeta_{jk}^{(i)} xy \end{pmatrix}. \quad (2.5)$$

A global transformation $T^{(i)}$ can be defined by combining all the local bilinear transformations. Since a bilinear transformation maps horizontal and vertical lines into straight lines, it transforms a rectangle into a quadrilateral. One can prove that the local bilinear transformation can be completely determined by the coordinates of the four transformed vertices defining the quadrilateral. Therefore, instead of considering the coefficients defining the bilinear transformations as variables, we consider as variables the coordinates of the transformed vertices

$$\begin{pmatrix} u_{jk}^{(i)} \\ r_{jk}^{(i)} \end{pmatrix} = z_{jk}^{(i)} = T^{(i)}(v_{jk}^{(i)}) = T^{(i)} \begin{pmatrix} s_j^{(i)} \\ t_k^{(i)} \end{pmatrix}. \quad (2.6)$$

Figure 2 shows a rectangle under a bilinear transformation.

For any point v inside the rectangle, we compute $\lambda, \mu \in [0, 1]$ as the horizontal and vertical ratios of v inside the rectangle, as indicated in the figure. The transformed point z can thus be computed as

$$z = T_{jk}(v) = (1 - \lambda)(1 - \mu)\,z_{jk} + \lambda(1 - \mu)\,z_{j+1,k} + (1 - \lambda)\mu\,z_{j,k+1} + \lambda\mu\,z_{j+1,k+1}. \quad (2.7)$$
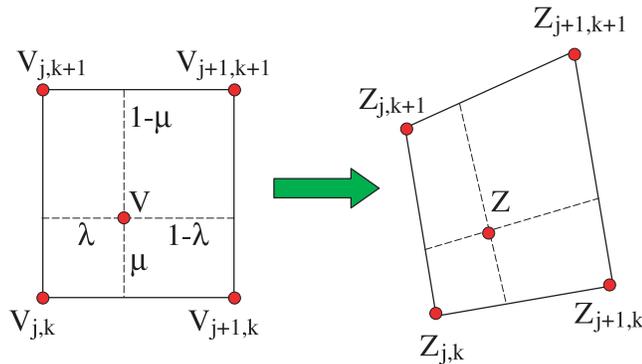

FIG. 2.   A rectangle under a bilinear transformation.

We need to align all the source gels through forward transformation to an ideal reference gel, so that every set of landmarks $L_{1l}, \ldots, L_{Ml}$ will be superimposed on an ideal landmark $L_l = (x_l, y_l)^T$ in the reference gel image, within some allowed error tolerance ϵ. The ideal landmarks L_l on the reference image are also considered as unknowns. This is enforced by the following constraints:

$$\|T^{(i)}_{m(i,l),n(i,l)}(L_{il}) - L_l\|_\infty \le \epsilon, \; i = 1, \ldots, M, \; l = 1, \ldots, N, \tag{2.8}$$

where $\| \bullet \|_\infty$ is the l_∞−norm, $\|(z_1, z_2)^T\|_\infty = max\{|z_1|, |z_2|\}$, and $(m(i,l), n(i,l))$ are the indices of the rectangle containing L_{il},

$$L_{il} \in \Omega^{(i)}_{m(i,l),n(i,l)}.$$

As shown in (2.7), $T^{(i)}_{m(i,l),n(i,l)}(L_{il})$ can be written as a linear combination of the transformed vertices defining the corresponding quadrilateral. Since $\|(z_1, z_2)^T\|_\infty \le \epsilon$ is equivalent to $-\epsilon \le z_1 \le \epsilon$, $-\epsilon \le z_2 \le \epsilon$, (2.8) represents a set of linear inequality constraints in the unknown variables $u^{(i)}_{jk}$, $r^{(i)}_{jk}$, x_l, y_l.

Since the ideal landmark L_l is representative of the family of M landmarks $L_{ll}, \ldots, L_{Ml}$, it should lie in a certain neighborhood of the geometric center

$$\overline{L}_l = \frac{1}{M} \sum_{i=1}^M L_{il}$$

of this family. Therefore we impose an additional set of linear inequality constraints of the form

$$\|L_l - \overline{L}_l\|_\infty \le E, \; l = 1, \ldots, N, \tag{2.9}$$

where E is a given error tolerance.

Finally, in order to avoid overlapping of different quadrilaterals after transformations, we impose the following constraints

$$|u^{(i)}_{jk} - u^{(i)}_{j+1,k}| \le \eta^x \Delta x^{(i)},$$

$$|r^{(i)}_{jk} - r^{(i)}_{j,k+1}| \le \eta^y \Delta y^{(i)}, \tag{2.10}$$

where $\eta^x, \eta^y \in (0, 1)$ are constants depending on the application. In our numerical experiments, we set $\eta^x = \eta^y = 0.5$.

The global piecewise bilinear transformation $T^{(i)}$ is globally continuous since local transformations from adjacent rectangles have the same values at common boundaries and vertices. However, it is not globally smooth (with continuous derivative). We want to determine the unknown 2D vectors $z^{(i)}_{jk}$, L_l, $i = 1, \ldots, M$, $j = 1, \ldots, p_i$, $k = 1, \ldots, q_i$, $l = 1, \ldots, N$, such that they satisfy the above constraints and the resulting transformations $T^{(1)}, \ldots, T^{(M)}$ have minimal curvatures and are as close as possible to the identity function. In this way, the warping functions $T^{(i)}$ will optimally align the family of gels $\mathcal{I}^{(1)}, \mathcal{I}^{(2)}, \ldots, \mathcal{I}^{(M)}$ to the ideal gel $\mathcal{I}$ without introducing unnecessary deformations. Therefore, from all possible variables that satisfy our constraints, we will determine a set of variables that minimize a quadratic objective function of the form

$$\mathcal{O} = w_1 \mathcal{R} + w_2 \mathcal{S} + w_3 \mathcal{T}, \tag{2.11}$$

where

$$\mathcal{R} = \sum_{i=1}^{M} \left(\sum_{j=2}^{p_i} \sum_{k=1}^{q_i+1} \left\| \frac{z_{j+1,k}^{(i)} + z_{j-1,k}^{(i)} - 2z_{jk}^{(i)}}{(\Delta x^{(i)})^2} \right\|^2 + \sum_{j=1}^{p_i+1} \sum_{k=2}^{q_i} \left\| \frac{z_{j,k+1}^{(i)} + z_{j,k-1}^{(i)} - 2z_{jk}^{(i)}}{(\Delta y^{(i)})^2} \right\|^2 \right), \qquad (2.12)$$

$$\mathcal{S} = \sum_{i=1}^{M} \left(\sum_{j=1}^{p_i} \sum_{k=1}^{q_i+1} \left\| \frac{r_{j+1,k}^{(i)} - r_{jk}^{(i)}}{(\Delta x^{(i)})^2} \right\|^2 + \sum_{j=1}^{p_i+1} \sum_{k=1}^{q_i} \left\| \frac{u_{j,k+1}^{(i)} - u_{jk}^{(i)}}{(\Delta y^{(i)})^2} \right\|^2 \right), \qquad (2.13)$$

$$\mathcal{T} = \sum_{i=1}^{M} \sum_{j=1}^{p_i+1} \sum_{k=1}^{q_i+1} \| z_{jk}^{(i)} - v_{jk}^{(i)} \|^2. \qquad (2.14)$$

Here w_1, w_2, and w_3 are constant weights and $\| \bullet \|$ denotes the l_2 norm, $\|(z_1, z_2)^T\| = z_1^2 + z_2^2$. The term $\mathcal{R}$ in the objective function measures the global curvature of the family of transformations $T^{(1)}, \ldots, T^{(M)}$, while $\mathcal{T}$ measures the distance of this family to the identity transformation. The middle term $\mathcal{S}$ measures the distance from the transformed grid composed of quadrilaterals, to a grid composed of rectangles parallel to the coordinate axes.

In conclusion, given the rectangular grid (2.1), and the family of landmarks L_{il}, $i = 1, \ldots, M, l = 1, \ldots, N$, we determine the ideal landmarks $L_1, \ldots, L_N$, and the forward transformations $T^{(1)}, \ldots, T^{(M)}$ by solving the following quadratic programming (QP).

$$\min_{z_{jk}^i, L_l} \quad \mathcal{O} \qquad (2.15)$$

$$\text{subject to} \quad \text{constraints (2.8), (2.9), and (2.10).}$$

There are $2 \sum_{i=1}^{M} (p_i + 1)(q_i + 1) + 2N$ variables in QP (2.15), which is almost four times smaller than the number of variables from the optimization problem constructed using the method in Potra et al. (2004) for the same grid. Nevertheless, in case of large families of gels, only a relatively coarse grid can be used with the forward transformations. In case of small families, we could use the hierarchical grid (multiresolution) approach of Potra et al. (2004), and refine the grid until some desired accuracy requirements are met. However, it turns out that, even for small families, it is advantageous to use forward transformations on a relatively coarse grid in order to obtain the ideal landmarks and the approximate size of the ideal gel, and then to use inverse transformations for better pair-wise alignment to the ideal gel on a sequence of finer and finer grids, as described in the following section.

2.2. Inverse transformations

Assuming that we have already determined an ideal reference gel image $\mathcal{I}$ with the ideal landmarks L_l, we can now decouple the original problem into M independent smaller problems that consist in aligning each gel to the ideal gel. More precisely, for each $i = 1, \ldots, M$, an inverse piecewise bilinear transformation is to be constructed for pair-wise alignment between $\mathcal{I}$ and $\mathcal{I}^{(i)}$.

We propose a multiresolution approach for finding an inverse bilinear transformation for source gel $\mathcal{I}^{(i)}$, based on constructing a sequence of increasingly finer partitions $\mathcal{P}_1^{(i)}, \mathcal{P}_2^{(i)}, \ldots$ on the ideal gel $\mathcal{I}$. Partition $\mathcal{P}_\kappa^{(i)}$ consists in dividing $\mathcal{I}$ into $p_{i,\kappa} \times q_{i,\kappa}$ rectangles where $p_{i,1}, p_{i,2}, \ldots, p_{i,\kappa}, \ldots$ and $q_{i,1}, q_{i,2}, \ldots, q_{i,\kappa}, \ldots$ are two increasing sequences of positive integers. In our application we take $p_{i,\kappa+1} = 2p_{i,\kappa}, q_{i,\kappa+1} = 2q_{i,\kappa}$, so that the number of rectangles increases by a factor of 4 at each grid refinement. Let us describe a typical partition. For simplicity we drop the indexes κ and i, and we assume that $\mathcal{I}$ is included in the rectangle

$\Omega = [\check{\tau}^x, \hat{\tau}^x] \times [\check{\tau}^y, \hat{\tau}^y]$. This rectangle is divided into $p \times q$ equal sub-rectangles

$$\Omega_{jk} = \left\{ z = \begin{pmatrix} x \\ y \end{pmatrix} \in R^2, \, s_j \leq x \leq s_{j+1}, \, t_k \leq y \leq t_{k+1} \right\}, \, j = 1, \ldots, p, \, k = 1, \ldots, q,$$

with vertices $v_{jk} = (s_j, t_k)^T$, where

$$s_j = \check{\tau}^x + (j-1)\Delta x, \, j = 1, \ldots, p+1, \tag{2.16}$$

$$t_k = \check{\tau}^y + (k-1)\Delta y, \, k = 1, \ldots, q+1, \tag{2.17}$$

and

$$\Delta x = \frac{\hat{\tau}^x - \check{\tau}^x}{p}, \quad \Delta y = \frac{\hat{\tau}^y - \check{\tau}^y}{q}. \tag{2.18}$$

We construct a global piecewise bilinear transformation $T^{(i)} : \mathcal{I} \to \mathcal{I}^{(i)}$ from a set of local bilinear transformations. We consider as variables the coordinates of the transformed vertices

$$\begin{pmatrix} u_{jk} \\ r_{jk} \end{pmatrix} = z_{jk} = T(v_{jk}) = T\begin{pmatrix} s_j \\ t_k \end{pmatrix}. \tag{2.19}$$

Following the ideas described in the previous subsection, we impose the following inequality constraints

$$|u_{jk} - u_{j+1,k}| \leq \eta^x \Delta x,$$
$$|r_{jk} - r_{j,k+1}| \leq \eta^y \Delta y, \tag{2.20}$$

and

$$\|T_{m(l),n(l)}(L_l) - L_{il}\|_\infty \leq \epsilon, \, l = 1, \ldots, N, \tag{2.21}$$

where $(m(l), n(l))$ are the indices of the rectangle containing L_l:

$$L_l \in \Omega_{m(l),n(l)}.$$

We then solve the following quadratic programming problem in order to construct the transformation $T^{(i)}$:

$$\min_{z_{jk}} \quad \tilde{w}_1 \tilde{\mathcal{R}} + \tilde{w}_2 \tilde{\mathcal{S}} + \tilde{w}_3 \tilde{\mathcal{T}} \tag{2.22}$$

$$\text{subject to} \quad \text{constraints (2.20), and (2.21),}$$

where

$$\tilde{\mathcal{R}} = \sum_{j=2}^{p} \sum_{k=1}^{q+1} \left\| \frac{z_{j+1,k} + z_{j-1,k} - 2z_{jk}}{(\Delta x)^2} \right\|^2 + \sum_{j=1}^{p+1} \sum_{k=2}^{q} \left\| \frac{z_{j,k+1} + z_{j,k-1} - 2z_{jk}}{(\Delta y)^2} \right\|^2, \tag{2.23}$$

$$\tilde{\mathcal{S}} = \sum_{j=1}^{p} \sum_{k=1}^{q+1} \left\| \frac{r_{j+1,k} - r_{jk}}{(\Delta x)^2} \right\|^2 + \sum_{j=1}^{p+1} \sum_{k=1}^{q} \left\| \frac{u_{j,k+1} - u_{jk}}{(\Delta y)^2} \right\|^2, \tag{2.24}$$

$$\tilde{\mathcal{T}} = \sum_{j=1}^{p+1} \sum_{k=1}^{q+1} \|z_{jk} - v_{jk}\|^2, \tag{2.25}$$

and $\tilde{w}_1$, $\tilde{w}_2$, $\tilde{w}_3$ are constant weights. If the desired accuracy or smoothness requirements are not met, we repeat the process on a finer partition $\mathcal{P}_{\kappa+1}$. Once the transformation $T^{(i)}$ is obtained, the intensity

values of the pixels on $\hat{\mathcal{I}}^{(i)} = T^{(i)}(\mathcal{I})$ are carried inversely from $\mathcal{I}$ using some interpolation technique. The resulting family of gel images $\hat{\mathcal{I}}^{(i)}$, $i = 1, \ldots, M$, are now hopefully well aligned.

The whole process is described by the following pseudo-code.

Algorithm

Given source gels $\mathcal{I}^{(i)}$ with landmarks L_{il},
(*forward transformations*)
compute ideal landmarks L_l and
estimate the size Ω of ideal reference gel $\mathcal{I}$ from (2.15);
(*inverse transformations*)
for $i = 1, \ldots, M$,
      start with partition $\mathcal{P}_0$: $p \times q$,
      repeat
            Compute s_j and t_k from (2.16) and (2.17);
            Obtain $T^{(i)}$ from the solution of (2.22);
            if   some stopping criterion is satisfied or
                    the maximum number of iterations is exceeded
                    Return;
            else
                    Refine the grid by setting $p = 2p$, $q = 2q$;
      compute $\hat{\mathcal{I}}^{(i)} = T^{(i)}(\mathcal{I})$.

Figure 3 shows a refinement step in the above algorithm. It is clear that the transformation after the refinement is smoother than before the refinement.

Remarks

1. The size of the ideal reference gel is estimated from the distribution of the ideal landmarks $L_l = (x_l, y_l)^T$, $l = 1, \ldots, M$, so that we are able to assign intensity values for all the pixels on $\hat{\mathcal{I}}^{(i)}$. In our application, the size of $\mathcal{I}$ is estimated as

$$[max(0, min(x)/1.1), max(x) * 1.1] \times [max(0, min(y)/1.1), max(y) * 1.1],$$

   where x and y are M-dimensional vectors, $x = (x_1, \ldots, x_M)^T$ and $y = (y_1, \ldots, y_M)^T$.
2. We use forward transformations for obtaining the ideal landmarks, because in this case we have linear constraints and the optimization problem reduces to a QP which can be solved efficiently using interior-point methods.
3. We choose to work with inverse transformations for pair-wise alignments because in this case it is easier to assign intensity values for $\hat{\mathcal{I}}^{(i)}$.
4. By using the argument from Potra et al. (2004), it follows that the cost of our multiresolution approach is only slightly bigger than the cost of solving the QP on the finest grid.

3. NUMERICAL EXPERIMENTS

Our data sets were taken from a gel image database made available to the public by Peter Lemkin (*http://binkley.ncifcrf.gov/users/lemkin*).

The first data set we tested is the Molt-4 data (*www.lecb.ncifcrf.gov/2DgelDataSets/index.html#MOLT-4*). It contains four gel images (512×512 pixels, 8-bit, 250 microns/pixel). 22 landmarks are picked on each gel. The second data set we tested is the human leukemias data (*www.lecb.ncifcrf.gov/2DgelDataSets/index.html#HEME-MALIG*). It contains 170 gel images (512×512 pixels, 8-bit, 250 microns/pixel).
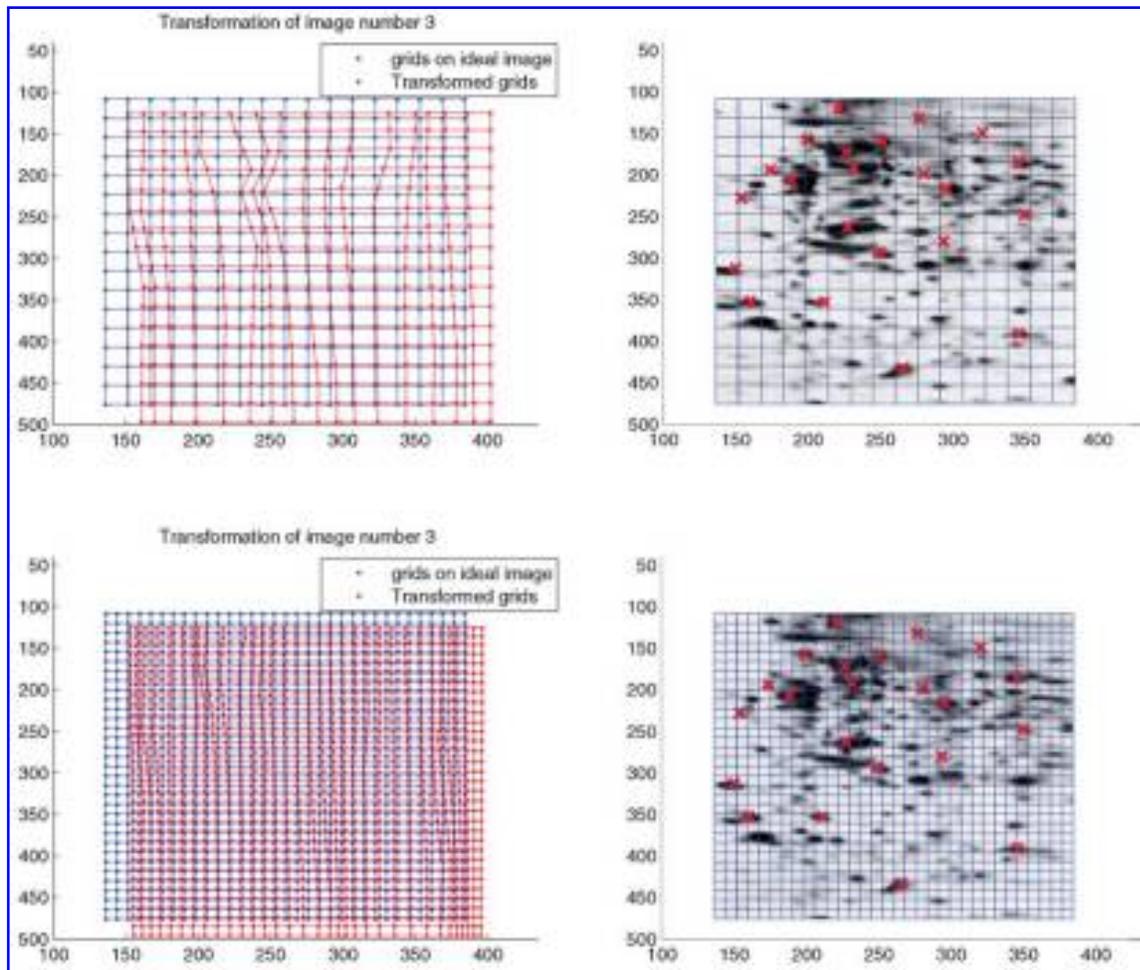
FIG. 3. The top two figures show the grid and gel image under an inverse piecewise bilinear transformation based on a 16×16 grid. The bottom two figures show the grid and the image under an inverse piecewise bilinear transformation based on a 32×32 grid (one refinement). Landmarks are shown in red crosses on the gel image.

For more details on this data see Lester et al. (1982, 1984). Most of the gel images contain 22 landmarks, while some images contain different numbers of landmarks. In order to have a set of compatible gel images, we picked only the images containing 22 landmarks. We thus have 123 gel images with 22 landmarks on each image.

It is very difficult to quantify the quality of an alignment by a simple mathematical formula. This is usually done by an expert practitioner through visual inspection. A simple but not necessarily very significant measure of the quality of alignment of images I and J is given by the normalized l_2-norm of the absolute difference:

$$SM = \sqrt{\frac{\sum_k (I_k - J_k)^2}{n}}, \tag{3.1}$$

where I_k and J_k represent the intensities of pixel k in image I and J respectively.

In our experiments, forward transformations were obtained based on a 16×16 grid. We took $\epsilon = 5$ (pixels) to find the forward transformations. The ideal positions of the landmarks were recorded and used to find a set of inverse transformations for each of the gel images. We took $\epsilon = 0$ (perfectly matching the ideal landmarks) to find the inverse transformations. In general, there could be different choices of stopping criteria in the multiresolution algorithm, based on either the change of the similarity measure,

or the size of the total curvature of the transformed grid. However, in the absence a "good" similarity measure, we decided to stop the algorithm by setting the maximum number of iteration equal to 2. Thus in our experiment we stopped at a 32×32 grid to get the inverse transformation.

The original code is written in Matlab and C. The QPs are solved by the interior point method based software package MOSEK (*www.mosek.com*).

Data Set 1. Experimental results for this data set are shown in Table 1. In order to have comparable results, the gray level of each image is scaled to the interval $[0, 255]$ before computing the similarity measure. We can see that the forward transformation improved the similarity significantly. Then, the inverse transformation further improved the similarity at a much lower computational cost. The effects of alignment are shown in Figure 4, which is the superimposition of the central part of the images from Figure 1.

Data Set 2. There are 123 gel images in this data set. Table 2 shows a sample result of superimposition of image 1 (gel-HM-001.gif) and image 3 (gel-HM-003.gif). The effects of alignment are shown in Figure 5. From the alignment data in Table 2, it seems that the two figures align very well. However, Figure 5 shows that there are some problems aligning the left bottom corner of the images. If we take a closer look at that region in Figure 6, with the landmarks shown as crosses, it is clear that we do not have enough accurate landmarks to properly cover that particular region.

TABLE 1. SIMILARITY MEASURE FROM NUMERICAL EXPERIMENTS
FOR DATA SET 1

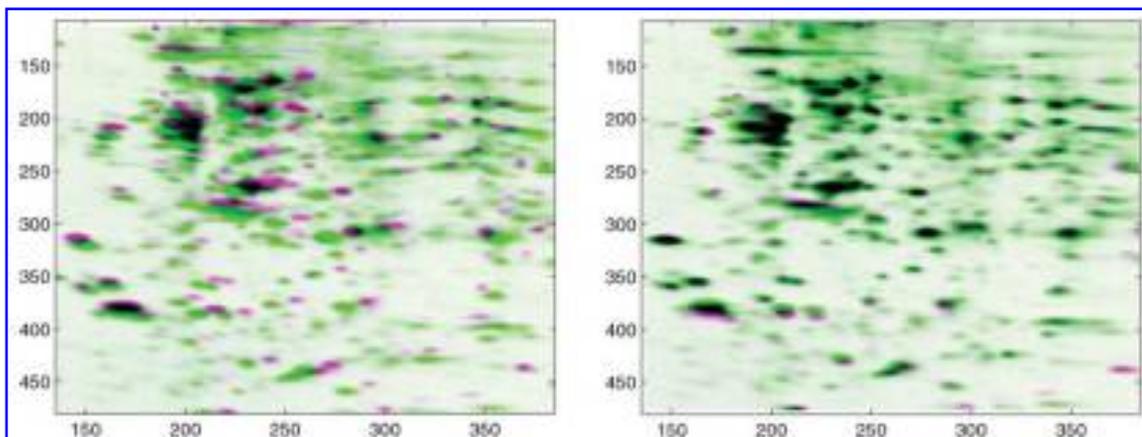|	*Original images*	*After fwd. trans.*	*After inv. trans.*
Image 1 vs. 2	41.17	24.33	14.19
Image 1 vs. 3	49.72	41.59	32.30
Image 1 vs. 4	34.30	25.13	22.63

FIG. 4. The superimposition of the center part of the images from Figure 1, after performing a forward piecewise bilinear transformation (left figure) followed by an inverse piecewise bilinear transformation (right figure).

TABLE 2. A SAMPLE EXPERIMENTAL RESULT FOR DATA SET 2: IMAGES 1 AND 3

	Original images	*After fwd. trans.*	*After inv. trans.*
Similarity measure	23.04	17.22	13.65
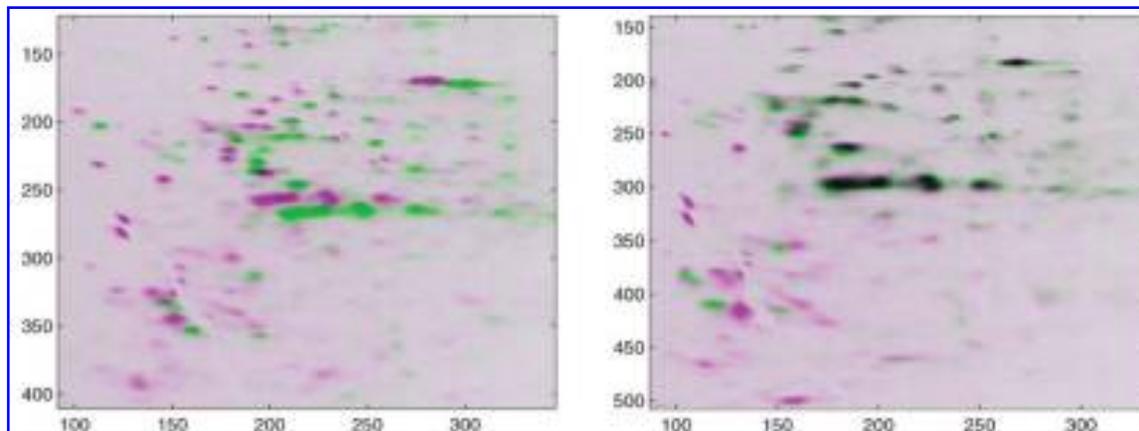
FIG. 5. The superimposition of a sample pair of gel images in data set 2. The left figure shows the superimposition of the source image 1 (gel-HM-001.gif) and source image 3 (gel-HM-003.gif). The right figure shows the superimposition of the two after alignment using piecewise bilinear transformations.
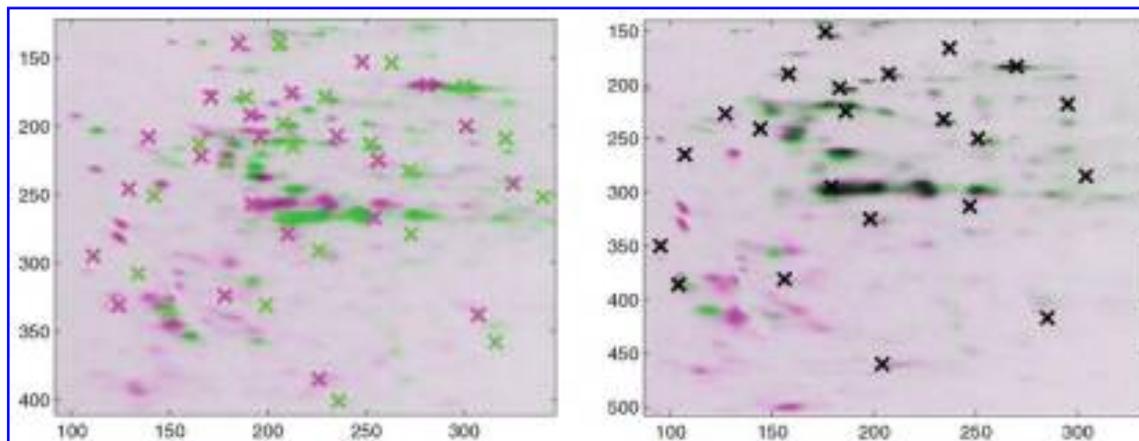
FIG. 6. The figures from Figure 5, with landmarks. The landmarks in the lower bottom corner may not have been very accurately picked.

4. CONCLUSION

In this paper, we have presented a methodology for aligning families of 2D gels that does not rely on choosing one of the gels as reference, but constructs an ideal gel and the corresponding warping transformations from the solution of a quadratic programming problem. We have implemented this methodology by using a combination of forward and inverse continuous piecewise bilinear transformations. The inverse transformation is obtained on hierarchical grids and has optimized global curvature. Moreover, our approach has a lower computational than the approach in Potra et al. (2004), and has better performance in assigning intensity values for the aligned images.

It is not very clear how to measure the quality of the alignment. At present, this is mostly done by visual inspection by a specialist. However, it would be very beneficial if one could derive a satisfactory objective quantitative measure for the quality of gel image alignment. This would open the possibility of designing efficient algorithms that can automatically align large families of gels (with or without preassigning landmarks), removing thus the bottleneck for very large scale proteomics studies.

ACKNOWLEDGMENT

REFERENCES

Dowsey, A.W., Dunn, M.J., and Yang, G.-Z. 2003. The role of bioinformatics in two-dimensional gel electrophoresis. *Proteomics* 3, 1567–1596.

Glasbey, C.A., and Mardia, K.V. 1998. A review of image warping methods. *J. Appl. Statist.* 25, 155–171.

Gustafsson, J.S., Blomberg, A., and Rudemo, M. 2002. Warping two-dimensional electrophoresis gel images to correct for geometric distortions of the spot pattern. *Electrophoresis* 23, 1731–1744.

Kaczmarek, K., Walczak, B., de Jong, S., et al. 2003. Comparison of image-transformation methods used in matching 2D gel electrophoresis images. *Acta Chromatogr.* 13, 7–21.

Klose, J. 1975. Protein mapping by combined isoelectric focusing and electrophoresis: a two-dimensional technique. *Humangenetik* 26, 231–234.

Lester, E.P., Lemkin, P., and Lipkin, L. 1982. A two-dimensional gel analysis of autologous t and b lymphoblastoid cell lines. *Clin. Chem.* 28, 828–839.

Lester, E.P., Lemkin, P., and Lipkin, L. 1984. Protein indexing in leukemias and lymphomas. *Ann. NY Acad. Sci.* 428, 158–172.

O'Farrell, P.H. 1975. High resolution two-dimensional electrophresis of proteins. *J. Biol. Chem.* 250, 4007–4021.

Potra, F.A., Liu, X., Seillier-Moiseiwitsçh, F., et al. 2004. Protein image alignment via global and segmented local forward affine transformations. *J. Comp. Biol.* 13, 614–630.

Potra, F.A., and Wright, S.J. 2000. Interior-point methods. *J. Comput. Appl. Math.* 124, 281–302.

Salmi, J., Aittokallio, T., Westerholm, J., et al. 2002. Hierarchical grid transformation for image warping in the analysis of two-dimensional electrophoresis gels. *Proteomics* 2, 1504–1515.

Veeser, S., Dunn, M.J., and Yang, G.-Z. 2001. Multiresolution image registration for two-dimensional gel electrophoresis. *Proteomics* 1, 856–870.

Voss, T., and Haberl, P. 2000. Observations on the reproducibility and matching efficiency of two-dimensional electrophoresis gels: consequences for comprehensive data analysis. *Electrophoresis* 21, 3345–3350.

Address correspondence to:
Dr. Florian A. Potra
Department of Mathematics and Statistics
UMBC
1000 Hilltop Circle
Baltimore, MD 21250

E-mail: potra@math.umbc.edu